

Quantitative relationship between microstructural factors and fatigue life of Ti-5Al-2Sn-2Zr-4Cr-4 Mo (Ti-17) fabricated using a 1500-ton forging simulator

M. Niinomi^{1,2,3,4, 5}, T. Akahori¹, M. Nakai⁶, Y. Koizumi³, A. Chiba², T. Nakano³, T. Kakeshita⁷,
Y. Yamabe-Mitarai⁸, S. Kuroda⁸, N. Motohashi⁸, Y. Itsumi⁹, and T. Choda⁹

1. Department of Science and Technology, Meijo University, Nagoya 468-8502, Japan.
2. Institute for Materials Research, Tohoku University, Sendai 980-5377, Japan.
3. Department of Materials and Manufacturing Science, Graduate School of Engineering, Osaka University, Osaka 565-0871, Japan.
4. Institute of Materials and Systems for Sustainability, Nagoya University, Nagoya 464-8601, Japan.
5. Faculty of Chemistry, Materials and Bioengineering, Kansai University, Osaka 564-860, Japan.
6. Department of Mechanical Engineering, School of Science and Engineering, Kindai University, Osaka 577-8502, Japan
7. Faculty of Engineering, Fukui University of Technology, Fukui 910-8505, Japan.
8. National Institute for Materials Science (NIMS), Tsukuba 305-0047, Japan.
9. Kobe Steel, LTD., Kobe 675-0023, Japan.

Abstract

The microstructures, tensile properties, and fatigue lives of the forged Ti-17 using a 1500-ton forging simulator subjected to different solution treatments and a common aging treatment under both load- and strain-controlled conditions to evaluate high cycle fatigue and low cycle fatigue lives, respectively were examined. Then, the tensile properties, microstructures, and relationships between fatigue lives and the microstructural factors were discussed.

The fatigue limit under load-controlled conditions increases with increasing solution treatment temperature up to 1143 K, which is in the ($\alpha + \beta$) region. However, it decreases with further increase in the solution treatment temperature to 1203 K in the β region. The fatigue ratio at fatigue limit is increasing with decreasing solution treatment temperature, namely increasing the volume fraction of the primary α phase, and it relates well qualitatively with the volume fraction of the primary α phase when the solution treatment temperature is less than the β transus temperature. The fatigue life under strain-controlled conditions to evaluate the low cycle fatigue life increases with decreasing solution treatment temperature, namely increasing the volume fraction of the primary α phase. The fatigue life under strain-controlled conditions to evaluate the low cycle fatigue life relates well quantitatively with the tensile true strain at breaking of the specimen and the volume fraction of the primary α phase for each total strain range.

1. Introduction

The amount of usage for commercial aircrafts is recently rapidly increased because CFRP (carbon fiber reinforced plastics) is used for air frame structures [1]. On the other hand, titanium alloys are used not only in air frames, but also in jet engine components such as fans and compressor disks, which function at relatively low temperatures up to 673 K. Ti-5Al-2Sn-2Zr-4Cr-4 Mo (Ti-17), which is a age hardenable β -rich two-phase ($\alpha + \beta$) -titanium alloy, was developed to reduce the titanium components in the early 1970s in the USA and registered as AMS 4955; it exhibits greater strength, crack propagation resistance, and creep resistance compared with those of Ti-6Al-4V at intermediate temperatures. Ti-17 is β -forged to achieve high fracture toughness [2, 3, 4]. Notably, fatigue endurance is one of the important factors for the aforementioned engine components. The investigation of fatigue properties of Ti-17 by focusing on their relation with microstructural factors is highly significant. In particular, it is important to consider the quantitative relationship between fatigue properties and microstructural factors during the fatigue life estimation of engine components made of Ti-17. Therefore, in this study, the fatigue properties and microstructures of hot-forged disk-like Ti-17 samples were investigated to define the quantitative relationship between the fatigue properties and the microstructural factors in this study.

2. Experimental

Disk-like Ti-17 samples were fabricated using a 1500-ton forging simulator [5]. First, a Ti-17 ingot with a diameter of 120 mm and a height of 240 mm was forged at 1073 K. Then, a quarter of the forged disk-like sample was cut to prepare the tensile and fatigue specimens. For the preparation, the cut pieces were subjected to solution treatment (ST) at four different temperatures: 1063, 1123, 1143, and 1203 K followed by water quenching (WQ). The β transus temperature (T_{β}) of Ti-17 is around 1153 K; therefore, the ST temperature of 1203 K was slightly higher than T_{β} , but within the β region. However, the other three ST temperatures were lower than T_{β} , and in the ($\alpha + \beta$) region. Each sample was then subjected to an aging treatment at 893 K for 8h, followed by air cooling

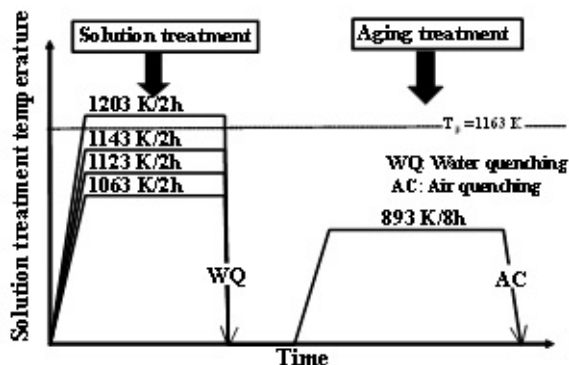


Fig. 1 Schematic drawing of heat treatment process carried out in this study.

(AC). The heat treatment processes are schematically shown in Fig. 1 [6]. The samples subjected to aging after the different STs were denoted as ST/1063 K, ST/1123 K, ST/1143 K, and ST/1203 K, according to the ST temperatures. Smooth round bar-shaped tensile specimens with a gage diameter of 7.0 mm, a gage length of 14 mm, and a total length of 34 mm, hour-glass shaped fatigue specimens with a minimum diameter of 3 mm and a length (without the gripping part) of 28 mm, and a total length of 52 mm for load-controlled fatigue tests, and smooth round bar fatigue specimens with a diameter of 3 mm, a gage length of 15 mm, and a total length of 52 mm for strain-controlled fatigue tests were machined from the aged samples. Tensile tests were carried out at a strain rate of 0.5%/min up to a strain of 5% and after that, a strain rate of 1.5%/min using an Instron-type testing machine with a capacity of 10 kN, at ambient temperature. Fatigue tests under load-controlled conditions to evaluate the high cycle fatigue life were carried out at a stress ratio (R) of 0.1 using an electro-hydraulic servo

fatigue testing machine with a capacity of 5 kN, at ambient temperature. The fatigue tests under strain-controlled conditions to evaluate the low cycle fatigue life were carried out at representatively selected total strain ranges of 1.05, 1.1, and 1.2, respectively using an electro-hydraulic servo fatigue testing machine with a capacity of 100 kN, at ambient temperature. Microstructural observations of the sample were carried out using an optical microscopy. Fatigue fracture surfaces were observed using a scanning electron microscopy (SEM).

3. Results and discussion

3.1 Microstructure

The microstructure of ST/1203 K exhibited equiaxed prior β grains composed of fine acicular α because it was subjected to ST at a temperature higher than T_{β} . On the other hand, microstructures of ST/1063 K, ST/1123 K, and ST/1143 K exhibited elongated prior β grains composed of two different microstructural feature regions: primary acicular α and fine spheroidal α regions as shown in Fig. 2. The primary acicular α region was predominant as compared with that of the fine spheroidal α region. Therefore, the authors focused on the primary acicular α region. The volume fraction of the primary α in the primary α region is shown in Table 1.

Table 1 Volume fractions of primary α phase.

Volume fraction (%)	Specimen		
	ST/1063 K	ST/1123 K	ST/1143 K
Primary α phase	47	24	6.1

3.2 Tensile Properties

Notably, the 0.2% proof stress and tensile strength increased with increasing ST temperature up to 1143 K (within the $(\alpha + \beta)$ region), but decreased with further increase in the ST temperature to 1203 K (within the β region). In addition, the elongation and reduction of area decreased with increasing ST temperature, and it became nearly 0 % corresponding to a ST temperature of 1203 K. Interestingly, the 0.2% proof stress and tensile strength of ST/1203 K were equivalent. Therefore, ST/1203 K was considered to be fractured in a very brittle manner.

3.3 Fatigue life under load-controlled conditions

Fatigue lives of ST/1063 K, ST/1123 K, ST/1143 K, and ST/1203 K under load-controlled conditions are shown in Fig. 3 [6] as a function of maximum cyclic stress (σ_{max})-number of cycles to failure (N_f) curves. The fatigue limit increases with increasing ST temperature up to 1143 K, corresponding to the $(\alpha + \beta)$ region; however, it decreases with further increase in the ST temperature to 1203 K. Accordingly, ST/1203 K exhibits the lowest fatigue limit.

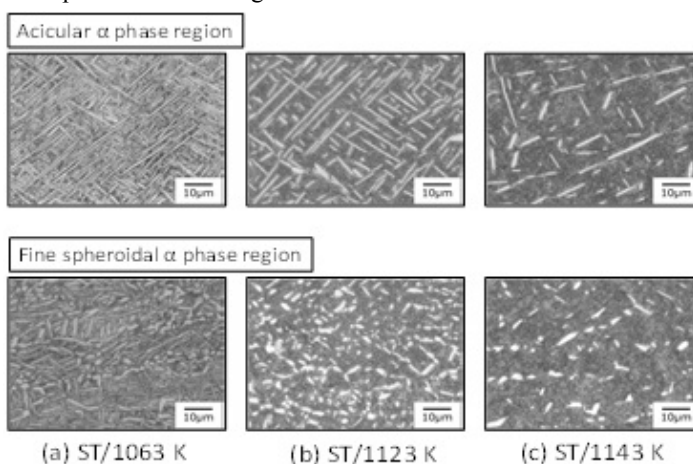


Fig. 2 Highly magnified optical micrographs of acicular and fine spheroidal phase regions in (a) ST/1063 K, (b) ST/1123 K, and (c) ST/1143 K.

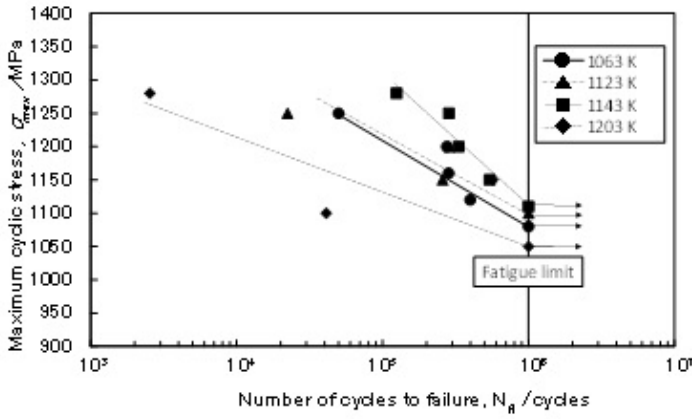


Fig.3 Maximum cyclic stress (s_{max})-number of cycles to failure (N_f) ($S-N_f$) curves showing fatigue lives of ST/1063 K, ST/1123 K, ST/1143 K, and ST/1203 K under load-controlled conditions.

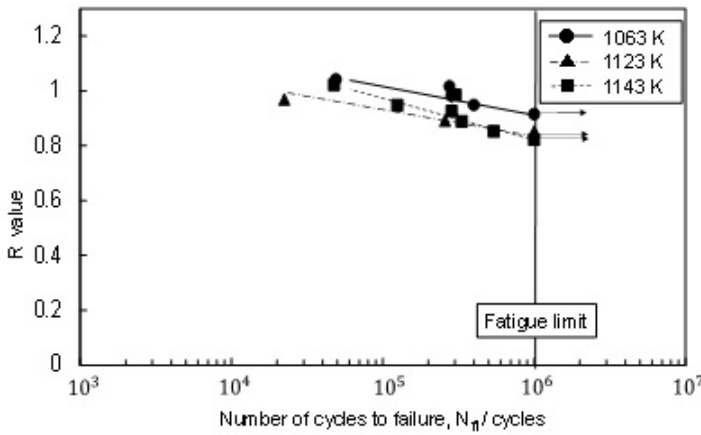


Fig. 4 Relationship between fatigue ratio (R) values of ST/1063, ST/1123, and ST/1143 and number of cycles to failure (N_f) under load-controlled fatigue conditions.

total strain range ($\Delta\epsilon_t$ %), and the number of cycles to failure (N_{fs}), of ST/1063 K, ST/1123 K, ST/1143 K, and ST/1203 K. Contrary to the trend recognized in the fatigue life under load-controlled conditions (fatigue limit), the fatigue life under strain-controlled conditions increases with decreasing ST temperature in ST/1063 K, ST/1123 K, and ST/1143 K. The fatigue life of ST/1203 under strain-controlled conditions is the worst as similar in the case of the fatigue life under load-controlled conditions.

N_{fs} , was found to be well related to the tensile true strain at the breaking of the specimen (ϵ_{tt}) as shown in Fig. 7 [6]. Therefore, the relationship between N_{fs} and ϵ_{tt} can be expressed by the following equation for each $D\epsilon_t$ [6].

$$\epsilon_{tt} = 0.6 \cdot 10^{-3} N_{fs}^{0.62} \quad \text{for } \Delta\epsilon_t = 1.05 \% \quad (2)$$

$$\epsilon_{tt} = 0.8 \cdot 10^{-3} N_{fs}^{0.56} \quad \text{for } \Delta\epsilon_t = 1.10 \% \quad (3)$$

$$\epsilon_{tt} = 2.5 \cdot 10^{-3} N_{fs}^{0.41} \quad \text{for } \Delta\epsilon_t = 1.2 \% \quad (4)$$

The morphology of the fatigue fracture surface of ST/1203 showing very brittle fatigue fracture surface was remarkably different from those of ST/1063 K, ST/1123 K, and ST/1143 K; the crack initiation mechanism of ST/1203 K is likely different from those of ST/1063 K, ST/1123 K, and ST/1143 K. The Ti-17 subjected to ST at a temperature over T_β is generally not appropriate for the practical applications.

Therefore, the fatigue ratios (σ_{max} at each number of cycles to failure / tensile strength) of ST/1063 K, ST/1123 K, and ST/1143 K having primary α phases are shown in Fig. 4 as a function of the number of cycles to failure. Then the fatigue ratio (R) values at the fatigue limits of ST/1063 K, ST/1123 K, and ST/1143 K were evaluated to be 0.92, 0.85, and 0.82, respectively. Therefore, ST/1063 K shows the greatest R value at the fatigue limit.

The R value at the fatigue limit was found to be related with the volume fraction of the primary α phase, V(%) as shown in Fig. 5 [6]. Therefore, the relationship between the R value and V(%) can be expressed by the following equation [6].

$$R = 0.80 \cdot e^{0.0029V(\%)} \quad (1)$$

3.4 Fatigue life under strain-controlled conditions

Figure 6 [6] shows the relationship between the

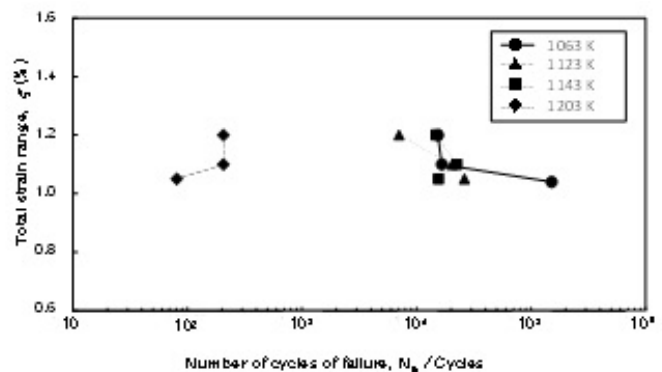


Fig.5 Relationship between total strain range (ϵ_t) and number of cycles to failure (N_{fs}) showing fatigue lives of ST/1063 K, ST/1123 K, ST/1143 K, and ST/1203 K under strain-controlled conditions.

ϵ_{ff} was also found to be quantitatively related to the volume fraction of the primary α phase. Therefore, N_{fs} for each $\Delta\epsilon_f$ can be also well quantitatively related to the volume fraction of the primary α phase.

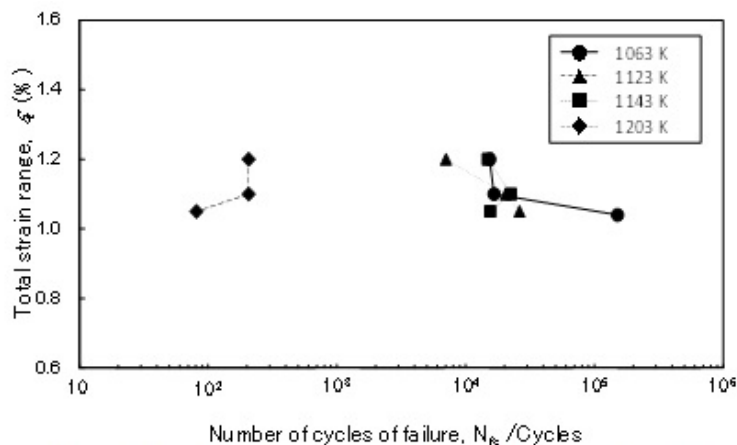


Fig.6 Relationship between total strain range (ϵ_f) and number of cycles to failure (N_{fs}) showing fatigue lives of ST/1063 K, ST/1123 K, ST/1143 K, and ST/1203 K under strain-controlled conditions.

Conclusions

1. The fatigue life under load-controlled conditions to evaluate the high cycle fatigue life

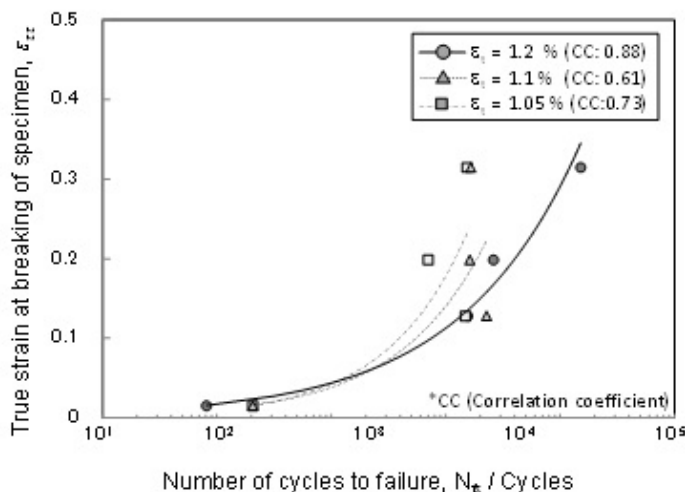


Fig. 7 Relationship between tensile true strain (ϵ_{ff}) at breaking of specimen obtained by tensile test and fatigue life under strain-controlled fatigue conditions, which is the number of cycles to failure (N_{fs}) for each total strain range.

increases with increasing solution treatment temperature up to 1143 K, which is in the ($\alpha + \beta$) region. However, it decreases with further increase in the solution treatment temperature to 1203 K in the β region.

2. The fatigue ratio at fatigue limit under load-controlled conditions increases with decreasing solution treatment temperature, namely increasing volume fraction of the primary α phase, and relates well qualitatively with the volume fraction of the primary α phase when the solution treatment temperature is less than the β transus temperature.
3. The fatigue life under strain-controlled conditions to evaluate low cycle fatigue life increases with decreasing solution treatment temperature, namely increasing the volume fraction of the primary α phase.
4. The fatigue life under strain-controlled conditions relates well quantitatively with the tensile true strain and the volume fraction of the primary α phase for each total strain range.

Acknowledgement

This work was partly supported by the Structural Materials for Innovation, Cross-ministerial Strategic Innovation Promotion Program, Cabinet Office, Government of Japan.

References

- [1] I. Inagaki, T. Takechi, Y. Shirai, N. Ariyasu, Nippon Steel & Sumitomo Metal Technical Report. (2014)106, 22-27.
- [2] T. K. Redden, in: Beta titanium alloys in the 1980's, eds. R. R. Boyer and H. W. Rosenberg, AIME, Warrendale, PA, USA, (1984), pp. 239-254.
- [3] Titanium alloys, in: Materials properties hand book, eds. R. Boyer, G. Weisch, and E. W. Collings, ASM Int., Materials Park, OH, USA, (1994), pp. 453-463.
- [4] J. Xu, W. Zeng, Z. Jia a, X. Sun, J. Zhou, J. Alloys and Compounds. 618 (2015) 343-348.

- [5] Y. Yamabe-Mitarai, *Bul. Iron and Steel Inst. (Ferrum)*, 22 (2017) 480-486.
- [6] M. Niinomi, T. Akahori, M. Nakai, Y. Koizumi, A. Chiba, T. Nakano, T. Kakeshita, Y. Yamabe-Mitarai, S. Kuroda, N. Motohashi, Y. Itsumi, and T. Choda., *Mater. Trans.* accepted.